Journal of Controlled Release 304 (2019) 75–89

Contents lists available at ScienceDirect

Journal of Controlled Release

journal homepage: www.elsevier.com/locate/jconrel

Characterization of branched poly(lactide-*co*-glycolide) polymers used in injectable, long-acting formulations

Justin Hadar[a], Sarah Skidmore[a], John Garner[a], Haesun Park[a], Kinam Park[a,b,*], Yan Wang[c], Bin Qin[c], Xiaohui Jiang[c]

[a] Akina, Inc., 3495 Kent Avenue, Suite A200, West Lafayette, IN 47906, USA
[b] Biomedical Engineering and Pharmaceutics, Purdue University, 206 S. Martin Jischke Drive, West Lafayette, IN 47907, USA
[c] Food and Drug Administration, Center for Drug Evaluation and Research, Office of Generic Drugs, 10903 New Hampshire Avenue, Silver Spring, MD 20993, USA

ARTICLE INFO

Keywords:
Branched PLGA
Star-shape PLGA
Sandostatin
Q1/Q2 sameness
Long-acting depot

ABSTRACT

Poly(lactide-*co*-glycolide) (PLGA) has been used in many injectable, long-acting depot formulations. Despite frequent use of PLGA, however, its characterization has been limited to measuring its molecular weight, lactide:glycolide (L:G) ratio, and end-group. These conventional methods are not adequate for characterization of unique PLGA polymers, such as branched PLGA. Glucose-initiated PLGA (Glu-PLGA) has been used in Sandostatin® LAR Depot (octreotide acetate for injectable suspension) approved by the U.S. Food and Drug Administration (FDA) in 1998. Glu-PLGA is a branched (also known as *star*-shaped) polymer and determining its properties has been challenging. It is necessary to develop methods that can determine and characterize the branching parameters of Glu-PLGA. Such characterization is important not only for the quality control of formulations, but also for developing generic parenteral formulations that are required to have the same excipients in the same amount (qualitative/quantitative (Q1/Q2) sameness) as their Reference Listed Drug (RLD).

In this study, an analytical technique was developed and validated using a series of branched-PLGA standards, and it was used to determine the branching parameters of Glu-PLGA extracted from Sandostatin LAR, as well as Glu-PLGAs obtained from three different manufacturers. The analytical technique was based on gel-permeation-chromatography with quadruple detection systems (GPC-4D). GPC-4D enabled characterization of Glu-PLGA in its concentration, absolute molecular weight, hydrodynamic radius and intrinsic viscosity. The plot of the branch units per molecule as a function of molar mass provides a unique profile of each branched PLGA. The Mark-Houwink plots were also used to distinguish different Glu-PLGAs. These ensemble identification methods indicate that the branch units of Glu-PLGAs extracted from Sandostatin LAR range from 2 (i.e., linear) at the lower end of the molecular weight to < 4 for the majority (94%) of Glu-PLGA.

1. Introduction

Poly(lactide-*co*-glycolide) (PLGA) has been widely used in injectable, long-acting depot formulations approved by the U.S. Food and Drug Administration (FDA) [1–9], and intensive research has been done on utilizing PLGA to develop various depot formulations and to understand the drug release mechanisms [10–24]. PLGA is synthesized by ring-opening polymerization of lactide and glycolide monomers, and this is usually done by using stannous octoate as a catalyst activating hydroxyl moieties to initiate ring-opening polymerization [25]. The hydroxyl moiety is attached to the growing PLGA chain by an ester bond. In the simplest manifestation, water itself can serve as the initiator to form PLGAs with a free-acid end-cap. Other alkyl hydroxyl initiators, such as dodecanol, result in alkyl ester PLGAs [26]. A wide array of PLGA polymers can be generated by controlling the access to hydroxyl initiation sites. For example, the use of hydroxyl end-capped poly(ethylene glycol) (PEG) enables the generation of block copolymers of PEG and PLGA (PEG-PLGA). Additionally, the hydroxyl groups of glucose and cyclodextrin can be utilized as initiators to synthesize subsequent PLGA-ester conjugates [27,28].

For a proposed generic product to be approved under an abbreviated new drug application (ANDA), it must demonstrate bioequivalence to the reference listed drug (RLD) [29]. For a parenteral drug product, where most of PLGA based long-acting formulations fall into this category, establishing bioequivalence has further requirements on inactive ingredients of the formulation, known as Q1 and Q2. Q1 means qualitative sameness between generic and RLD products with respect to composition of the components,

* Corresponding author at: Akina, Inc., 3495 Kent Avenue, Suite A200, West Lafayette, IN 47906, USA.
E-mail address: pk@akinainc.com (K. Park).

https://doi.org/10.1016/j.jconrel.2019.04.039
Received 16 March 2019; Received in revised form 24 April 2019; Accepted 28 April 2019
Available online 02 May 2019
0168-3659/

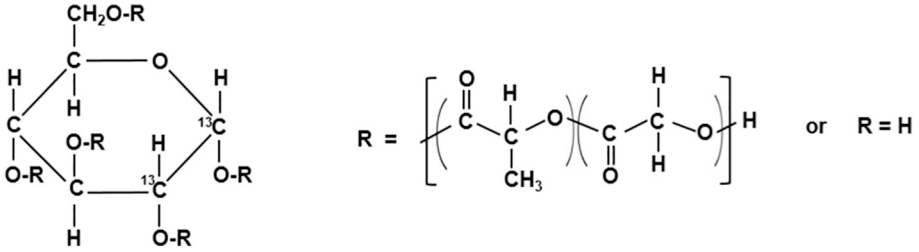

Fig. 1. Structure of Glu-PLGA. R represents either PLGA or hydrogen.

and Q2 represents quantitative similarity of each component [30]. Determining sameness of PLGA polymer, especially Glu-PLGA, remains a challenge for the regulatory authorities and for the generic drug industry. The goal of this work is to lay a foundational pathway for establishing Q1 (qualitative sameness) between the Glu-PLGA in RLD (Sandostatin® LAR) and any subsequent proposed generics.

Linear PLGAs can be readily characterized by determining the lactide:glycolide (L:G) ratio, molecular weight, end-cap [29], and uniformity of L:G arrangement [30]. Star-shaped or branched PLGAs were also prepared and characterized [20,22,31,32], but the method of determining the branch numbers per molecule has not been established yet. Traditional methods of measuring the molecular weight cannot provide information on the branch units per molecule. Glucose-initiated PLGA (Glu-PLGA) branched polymers have been used in Sandostatin LAR, an injectable long-acting formulation. Fig. 1 shows a schematic example of Glu-PLGA. There are potentially 5 sites for esterification which leads to a wide range of variations in branch formations. Glucose itself may also undergo ring-opening into an open-chain form.

Glucose, as with other simple sugars, is well known to undergo a caramelization reaction, a series of non-specific 'browning' reactions which change the structure and appearance of the sugar with heating [33]. These reactions occur readily at high temperatures and compete against the activity of glucose as an initiator as it undergoes these side reactions which act to modify or destroy the molecule before it can serve as an initiation site for PLGA formation. This reduces the glucose content within the polymer, but its extent is not known and its effect on the branching nature of the structure remains to be elucidated.

Gel-permeation chromatography (GPC) is frequently used to estimate the molecular weight of polymers based on the molecular weight standards. The separation of polymers by GPC is not entirely reliant on molecular weight, but rather on the hydrodynamic size of polymer molecules [34]. GPC can be combined with multi-angle laser light scattering (MALLS), viscometer, and refractive-index (*dn/dc*) detection for the universal calibration [35], and it allows determination of shape-factor and branching parameters for high molecular weight polymers with strong *dn/dc* [36,37]. To date, however, the branch units of star-shaped PLGAs has not been determined.

In this research, a series of branched-PLGA standards were prepared using simple multifunctional initiators which do not undergo side-reactions. These standards were used to develop and validate a GPC-based method for the determination of branch units of PLGA polymers. The method was applied to a series of commercially-available GMP-grade Glu-PLGAs, as well as the Glu-PLGA extracted from Sandostatin LAR depot formulation. In addition, ^{13}C-labeled glucose was used to synthesize Glu-PLGA and to track the presence of the glucose molecule by nuclear magnetic resonance (NMR) during the synthesis and subsequent hydrolysis of Glu-PLGA.

2. Experimental

2.1. Materials

Stannous octoate (SnOct), glucose, toluene, 1,2 hexanediol, trimethylolpropane, pentaerythritol, adonitol, activated charcoal, and dipentaerythritol were purchased from Sigma-Aldrich. Dichloromethane (DCM), tetrahydrofuran (THF), acetone (ACE), acetonitrile (ACN) and hexane were purchased from Fisher Scientific. Ethanol (200 proof) was obtained from Decon Laboratories, Inc. Lactide and glycolide were purchased from Ortec, Inc. and used as received. ^{13}C-labeled glucose was purchased from Cambridge Isotopes. Glu-PLGA was kindly provided by Corbion (Lenexa, KS), and also purchased from Evonik (Essen, Germany) and Lactel (Birmingham, AL). Stannous octoate was vacuum distilled before use, and all other reagents used as received. Desiccant packs (Aldrasorb), heat-exchanger plates, 0.220-in. acrylic sheet, and a water recirculator (Neslab RTE-7) were purchased from Sigma-Aldrich, Lytron, Shape Products, and Thermoscientific, respectively. Sandostatin LAR Depots (30 mg) were purchased through We Pharma (Morrisville, NC).

2.2. Synthesis of multi-arm PLGA standards

The standards for branched PLGAs are not available, and thus, they were synthesized by ring-opening polymerization [29]. Briefly, a multifunctional initiator for the desired number of arms was chosen. For this purpose, trimethylolpropane, pentaerythritol, adonitol, and dipentaerythritol were used for 3, 4, 5, and 6 arms, respectively, in accordance with the number of hydroxyls present on the molecules (Fig. 2). Additionally, 1,2 hexadiol was used to create a 'U-shaped' PLGA. The initiator was introduced into a round-bottom flask and azeotropically distilled from toluene under forced-argon to remove moisture. Monomers (lactide and glycolide) were initially dissolved in DCM at ~50% (*w/v*) and dried under vacuum to create a uniform mixture of both monomers. These monomers were then added to the initiator in predetermined quantities with stannous octoate in a 1:200 M ratio of catalyst to monomers. The mole of monomers to initiator was adjusted to obtain desired molecular mass. For Bent-low, Bent-High, 3-arm, 4-arm, 5-arm, and 6-arm the ratio of monomers to initiator hydroxyl were 117, 233, 115, 88, 70, and 58 to 1, respectively. Unless otherwise specified, all synthesis was done with DL lactide. The flask was vacuum sealed and the reaction proceeded at 150 °C for 8 h. The resultant crude polymer was washed with ethanol, dissolved in DCM, passed through a paper filter and precipitated in excess hexane to remove impurities. Subsequently, it was dried in a vacuum oven first at room temperature under deep vacuum (−78 mmHg) for approximately 1 week followed by vacuum drying at 50–60 °C for 2–3 weeks until reaching a constant mass.

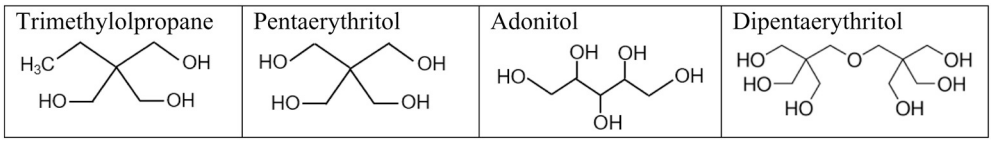

Fig. 2. Initiators used to make branched PLGAs with the branch units ranging from 3 to 6.

2.3. Synthesis of ^{13}C-labled Glu-PLGA (^{13}Glu-PLGA)

The ring-opening synthesis of PLGA by glucose was investigated in a step-wise manner. Glucose labeled with ^{13}C either at C1 and C2 or at all 6 carbons was used as an initiator. Briefly, small test batches were made by adding 100 mg of glucose into a 50 mL round-bottom-flask along with 6.4 g of D,L-lactide and 4.4 g of glycolide and 0.17 mL of stannous octoate. This was then vacuum purged and argon flushed multiple times, sealed and reacted in a vacuum at 130 °C for 8 h. Afterwards, a sample of crude polymer was withdrawn and assayed by NMR with the remaining crude polymer ethanol washed, DCM dissolved, filtered and precipitated in hexane. Subsequently, a sample was withdrawn and tested by NMR. The synthesized Glu-PLGA was subsequently decolorized by dissolution in 15 × volume of acetone and stirring with an equal mass of activated charcoal for 3 h followed by filtration removal of the charcoal and vacuum drying as described previously [38]. Similarly, a low-PLGA content version was generated by reducing the monomer concentration by 90%. Additionally, glucose and the stannous octoate catalyst were combined in absence of the monomers and heated to reaction temperatures under the same conditions to investigate the effect of reaction conditions on glucose.

2.4. Hydrolysis of ^{13}Glu-PLGA

For selected samples, PLGA branches were removed from previously made ^{13}Glu-PLGA by hydrolysis to extract the ^{13}C-labled glucose. The hydrolysis was accelerated by incubating the sample in an orbital agitating incubator (Southwest Science, Trenton, NJ) in 0.1 M NaOH solution at 50 °C with shaking at 100 RPM for 60 days. The resultant solution was concentrated by a rotary evaporator (Scilogix, Atkinson, NH) and analyzed by NMR.

2.5. Extraction and isolation of Glu-PLGA from Sandostatin LAR

Sandostatin LAR Depot (Novartis) 30 mg dose was obtained to analyze the composition of Glu-PLGA used in the formulation. Three different lots (lot# 356166, 356,510, and 357,028) of Sandostatin LAR were used. A vial containing 33.6 mg octreotide acetate, 566.4 mg PLGA, and 122.9 mg mannitol was removed from refrigeration and allowed to warm to room temperature. The vial content was transferred to two glass centrifuge tubes, resulting in approximately 350 mg of material in each tube. The sample was divided to allow for ample space in subsequent steps of extraction. Dry DCM (3 mL) was added to each tube before brief vortexing. The tubes were then placed in an incubator shaker at 100 RPM at 30 °C overnight to dissolve the polymer. On the following day the tubes were removed from the incubator shaker and vortexed again. The tubes were then centrifuged for five minutes at 3400 RPM. The resultant supernatant was then filtered through 0.22 μm PTFE syringe filter into new glass centrifuge tubes containing 8 mL of hexane to precipitate PLGA. The tubes were then filled with hexane, and left uncapped for 10 min to allow some DCM to evaporate. The tubes were then centrifuged for 5 min at 3400 RPM. Hexane was then decanted from the tubes leaving the precipitated sample behind. The tubes were left uncapped to allow a small amount of remaining hexane to evaporate. The PLGA sample was then dissolved by adding 3 mL DCM twice followed by 1.5 mL DCM with sonication after each solvent addition. All solvent additions were collected into two scintillation vials for a total of 7.5 mL of DCM in each vial. The vials were placed in light vacuum for 72 h and then placed in deep vacuum at 55 °C to completely dry before conducting analysis. The recovery of PLGA from this extraction process was 95.5 ± 4.7%.

2.6. Nuclear magnetic resonance (NMR) measurement

Each PLGA sample (5–10 mg) was dissolved in either deuterated chloroform ($CDCl_3$) or dimethyl-d_6 sulfoxide (DMSO-d_6) solvent (0.8 ml) and pipetted into a 7 in × 5 mm NMR tube. NMR scanning was performed using a Bruker AV-III-500-HD NMR spectrometer running TopSpin software (version 3.2) equipped with 5 mm BBFO *Z*-gradient cryoprobe Prodigy™ (the PINMRF group, Purdue University) for ^{1}H NMR. These spectra were used to determine the L:G ratio as previously described [29,39,40]. Briefly, the integration at 5.2 ppm (1H) and the integration at 4.8 ppm (2H) were compared to directly confirm the exact L:G ratio of each PLGA. The mole fraction lactide (M_L), peak integration lactide (P_L), and peak integration glycolide (P_G) were used as follows:

$$M_L = \frac{P_L}{P_L + \frac{P_G}{2}}$$

The ^{1}H-NMR spectra were carefully inspected to determine the esterification of the multifunctional initiator as described previously [41]. Briefly, the ratio of the peak intensity near 3.7 ppm was compared to the peak integration near 4.1 ppm, as these correspond to the free and esterified hydroxyls of the multifunctional initiator, respectively. ^{13}Glu-PLGA samples, both direct and from hydrolyzed solutions, were dissolved in DMSO-d_6 (0.8 ml) and analyzed by ^{13}C NMR. The ^{13}C-NMR spectra were obtained using a Bruker DRX500 NMR spectrometer equipped with a 5 mm *Z*-gradient TXI cryoprobe. Free induction decays were acquired using a ca. 30-degree RF pulse and power-gated WALTZ-16 1H decoupling (Bruker pulse-program zgpg30). A sweep width of ca. 241 ppm was employed and the data were acquired using 32 K complex data points. A 2-s relaxation delay was used and 4 K scans were acquired. The FIDs were processed with exponential multiplication (line-broadening factor of 3) prior to Fourier transformation without zero-filling. After manual phasing a baseline correction routine was applied. The number of scans for each polymer was adjusted to obtain a suitable signal-to-noise ratio and ranged between 1024–4096 scans. The number of scans for the ^{13}C-labeled glucose prior to the reaction was 128. An NMR post- analysis was performed using ACD/Spectrus Processor (2015 Pack 2, ACD Labs).

2.7. Gel-permeation chromatography using external standard molecular weights (GPC-ES)

The molecular weight of the polymers was determined as previously described [29,39,40]. Briefly, a Breeze-2 Water's GPC system comprising of a model 1515 isocratic pump, model 2707 autosampler, and model 2414 RI detector had a THF mobile phase pumped over three sequential GPC columns consisting of a Phenogel 5 μm packed 50 Å pore-size (300 mm × 7.5 mm), a Phenogel 5 μm packed 1 μm (10e4 Å) pore-size (300 mm × 7.5 mm, Phenomenex), and an Agilent Resipore 3 μm mixed pore-sizes (300 mm × 7.5 mm) columns. Each sample was injected 100 μL of a 2 mg/mL solution in DCM. Agilent EasiCal polystyrene standards were used to calibrate the system and the number average molecular weight, weight average molecular weight, and polydispersity was determined using Water's Empower software.

2.8. Osmometry

An Osmat-090 (Gonotec) pressure osmometer system was utilized with acetone as the solvent and a 20 kDa MWCO regenerated cellulose membrane as the osmometric barrier. The system pressure was calibrated using the hydrostatic pressure differential between the top and bottom of the instrument according to manufacturer's instructions. Each polymer was carefully prepared as a series of solutions ranging from 1 to 10 mg/mL. Each sample solution was flushed into the instrument a minimum of three times and then a measurement was taken after the pressure reached equilibrium (1–3 min). A series of four different concentrations were measured four times and averaged using the Osmomat software to extrapolate the molecular weight of accuratethe sample based on this data. This measurement was considered to be one singular data point.

During the measurements, the lowest fraction of polymer is removed. The smallest MWCO membrane available was 20 kDa, and thus, any molecules smaller than this can be removed. The reported accuracy by the manufacturer is ± 5 kDa. This means the method is less accurate than the difference between the M_n and M_w for these polymers. Like light scattering, it works better for very high molecular weight polymers. One advantage is there is no calibration or external standard so it is a good method to compare against GPC as an absolute method to make sure GPC results are valid.

2.9. Gel-permeation chromatography with quadruple detectors (GPC-4D)

The GPC-4D system consisted of an Agilent 1260 Infinity II HPLC system connected to Dawn Heleos II (MALLS) coupled to Dynapro Nanostar DLS via an optical cable, Optilab T-rEX (RI detector), and Viscostar III viscometer operated by Astra 7 software (Wyatt). The column used for separation was a linear gradient column (Tosoh Bioscience LLC, TSKgel GMH_{HR}-L, 7.8 mm × 30 cm).

The initial work was performed with THF as a mobile phase. This was mainly chosen because of the solvent's historical use for GPC analysis with polymers. This was also how the instrument was installed and qualified by the vendor. The vendor also qualified the system with polystyrene standards for light scattering detector normalization and inter-detector offset. Flow rates of 1.0, 0.6 and 0.3 ml/min were examined. By reducing the flow rate, the time the sample dwells in the flow cell of the light scattering detectors increases. Conversely, as the flow rate is increased, the response from the viscometer increases. Therefore, flow rate has a competing effect on the sensitivity of the two detectors. There is also a need to increase the run time when using a lower flow rate to allow all peaks to elute before the start of the next injection.

2.10. Determination of the incremental refractive index (dn/dc) of PLGA in different solvents

A critical factor in accurate determination of the molar mass using light scattering data is the incremental refractive index (*dn/dc*). This is in effect the contribution to absolute refractive index by the polymer in solution with respect to the concentration. Therefore, *dn/dc* is also solvent specific as the absolute refractive index varies from solvent to solvent. Accurate literature values for the *dn/dc* of PLGA are not available. To obtain the greatest accuracy from GPC-4D analysis, *dn/dc* was analyzed for specific PLGA/solvent combinations. Solutions of PLGAs with various molecular weights and L:G ratios were prepared in THF, acetone (ACE), and acetonitrile (ACN) at concentrations of 1, 2, 3, 4, and 5 mg/mL. Solvents were first filtered using 0.2 µm-filters, and then left stirring overnight with a loose cap to allow dissolved oxygen and atmospheric water to reach equilibration.

Solutions were directly perfused into the Wyatt T-rEX RI detector using a syringe pump. The refractive index was measured at 658.0 nm. After a baseline response of THF/ACE/ACN was established, PLGA solutions were measured as the concentration was changed from low to high. This was followed by blank THF/ACE/ACN to reestablish the baseline. Wyatt Astra software was used to calculate *dn/dc* for each set of PLGA solutions. Triplicate preparations of solutions were used to measure *dn/dc* and an average of triplicate analysis reported except where specified.

2.11. Determination of the solvent effect on data quality

The lower absolute refractive index of acetone and acetonitrile allows greater *dn/dc* response while maintaining an adequate chromatographic separation. Acetone was chosen over acetonitrile due to the fact that its solvent profile was available in the Astra software. The solvent profile in the Astra software contains values such as thermal expansion, viscosity, and the Rayleigh ratio which compensate for fluctuations in GPC system conditions. Once acetone was chosen as the best solvent, a signal alignment was performed using narrow molecular weight standards. This is necessary to compensate for time offsets between the multiple detectors as the sample transits the flow path. Normalization of the light scattering detectors was also necessary when switching solvents. The solubility of polystyrene in acetone was limited, and thus, poly(methyl methacrylate) (PMMA) standards were used for these procedures.

2.12. Determination of the sample load on data quality

The sample load was balanced by optimizing the sample concentration and injection volume. A greater sample loading yielded a greater response in all detectors. Ideally, a greater sample quantity could overcome limitations of the detector sensitivity for light scattering data. This, however, is counterproductive at a certain point, partially because of the column capacity and partly because of the saturation of the viscometer. At higher concentrations the signal from this detector fluctuates at the peak onset and conclusion, probably due to band broadening. This created variability in the viscosity and Mark-Houwink plots. A series of sample loads were tested by injecting varying concentrations of polymer in the sample at varying volumes, and the effect of the sample load on data quality was investigated.

2.13. Optimization of parameters determining the branch units

Astra 7 software has the option of determining branching properties of polymers, but it requires assigning a variety of user chosen parameters. These include a method of determining branching (radius, molar mass, or viscosity), model (trifunctional, tetra-functional, comb, or star), slice (monodisperse or polydisperse) and other parameters such as a drainage factor. The degree of branching can only be calculated when the molecular masses of branched and linear PLGAs overlap, i.e., in the region of the same molar masses. The equations used in calculating the branch unit/molecule are listed in Table 1. The branching ratio is calculated by comparing the mean square radii of gyration of branched and linear PLGAs measured by light scattering (g in Eq. (1)). The branching ratio can also be calculated using intrinsic viscosities (g' in Eq. (2)). The terms g and g' are related through Eq. (3), where "e" is the drainage factor. Once these values are obtained, the branch unit/molecule (B) can be calculated from a series of equations depending on the model of branching chosen (e.g., tri-functional, tetra-functional, comb, or star). Eq. (4) shows how the branching units are calculated based on the star model. There is a general rule that radii measured by light scattering must be > 1/20th of the wavelength of the scattered light. The R_b^2 and R_l^2 of the polymers were well below this limit, and thus, g' based on the intrinsic viscosity was chosen to determine the branching number.

2.14. Statistics

Unless otherwise specified, all quantitative experiments were performed in triplicate. All data shown is presented as average ± standard

Table 1
The equations to calculate the branching units per molecule from Astra 7 Users Guide (M1006 Rev.D). ($< R_b^2 >$ and $< R_l^2 >$ are mean square radius of gyration of branched and linear PLGA, respectively, having the same molecular weight, M. $[\eta]_b$ and $[\eta]_l$ are intrinsic viscosity of branched and linear PLGA, respectively, having the same molecular weight, M. "e" is the drainage factor that is specific for each PLGA, and "B" is the branch units per molecule.

Equation 1	Equation 2	Equation 3	Equation 4
$g = \left(\frac{< R_b^2 >}{< R_l^2 >}\right)_M$	$g' = \left(\frac{[\eta]_b}{[\eta]_l}\right)_M$	$g' = g^e$	$g = \frac{6B}{B^2 + 3B + 2}$

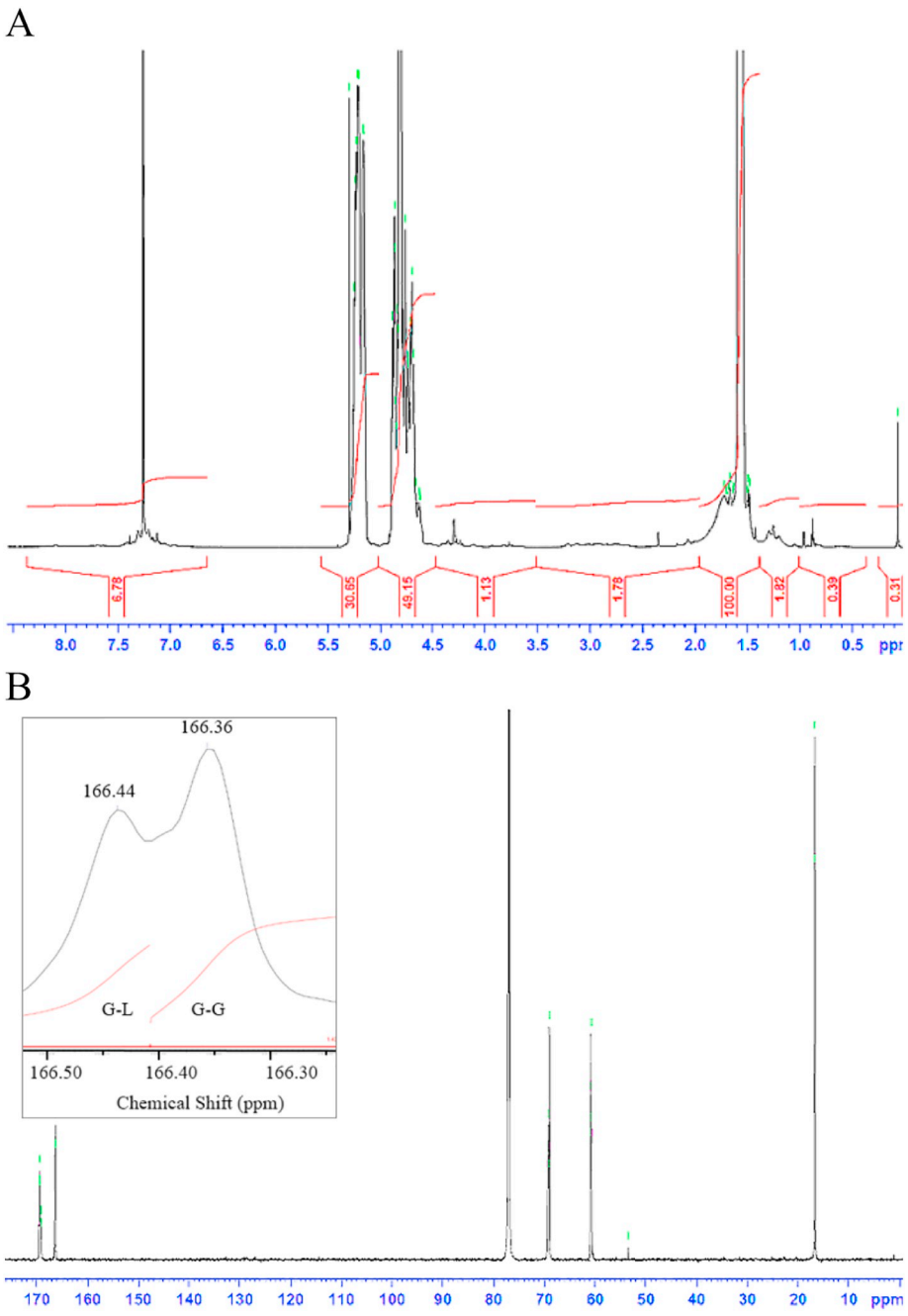

Fig. 3. ^{1}H-NMR (A) and ^{13}C-NMR (B) spectra of the PLGA extracted from Sandostatin LAR. The insert in (B) shows peaks at 166.36 and 166.44 ppm. No peaks ascribed to glucose are found from the ^{13}C-NMR (B).

deviation. Student's unpaired *t*-test was performed using GraphPad and results with $p < 0.05$ were considered significant.

3. Results

3.1. PLGA extracted from Sandostatin LAR: NMR characterization

Glu-PLGA extracted from Sandostatin LAR was characterized to enable comparison with Glu-PLGA in generic formulations. The PLGA extracted from Sandostatin LAR (lot# 356166) was characterized by NMR. Fig. 3A shows ^{1}H NMR and ^{13}C NMR spectra. The peak integrations at 4.8 ppm and 5.2 ppm (49.15 and 30.65, respectively) of the ^{1}H NMR spectrum (Fig. 3A) indicate that the L:G ratio of this particular Sandostatin LAR extract is 55.5:44.5. Measurement of three different Sandostatin LAR samples from two different lots (lot# 356166 and 356,510) showed the lactide content of 56.8 ± 1.2%. The ^{13}C NMR spectrum in Fig. 3B does not indicate the presence of glucose. All peaks are ascribed to PLGA. The absence of any peaks from glucose was a surprise, since it was known that Sandostatin LAR formulation consists of Glu-PLGA.

The distribution of lactide and glycolide in PLGA is expected to be random, but there may be blocks where glycolide monomers are present in sequence. The glycolide blockiness affects the PLGA solubility in organic solvents, and the blockiness (R_c) is determined by dividing the peak intensity of the glycolide-glycolide (G-G) carbonyl group (located at 166.36 ppm in Fig. 3B) by the peak intensity of the glycolide-lactide (G-L) carbonyl group (located at 166.44 ppm in Fig. 3B) [30]. The higher R_c value indicates higher blockiness, i.e., higher heterogeneity in the distribution of lactide and glycolide monomers. The R_c value of the PLGA extracted from Sandostatin LAR was determined to be 1.43.

Measurement of three different Sandostatin LAR samples from two different lots (lot# 356166 and 356,510) indicates the R_c value of 1.46 ± 0.07. This indicates that the glycolide-glycolide sequence is fairly prevalent along the polymer chain. This glycolide blockiness is one of the reasons that PLGAs with low L:G ratios have poor solubility in several solvents [42]. The information on the L:G ratio and blockiness does not provide any information on the PLGA molecular structure, e.g., linear or branched, and the number of branch units per glucose molecule, if branched. The information on the L:G ratio, however, is critical to the determination of the branch units of Glu-PLGA as described below.

3.2. Synthesis of branched PLGA Standards

To determine the branching number of Glu-PLGA, a series of standard polymers were generated and characterized by NMR and GPC using external standard molecular weights (GPC-ES). A series of polymers were also obtained commercially and characterized. The properties of the polymers are shown in Table 2 below.

The NMR spectra of the PLGAs with 3–6 arms (or branches), prepared using initiators in Table 2, were analyzed to determine esterification degree, and the peak assignments were based on previous publications [41,43,44].

The peaks relevant to the degree of esterification were integrated. The analysis indicated that for all synthesized branched polymer standards, the amount of free initiator (unreacted hydroxyls) was near or below the detectable range of the spectrometer indicating minimal presence of unreacted hydroxyl groups. This does not necessarily rule out the possible presence of linear, acid-ended PLGA polymers mixed in with the branched material. It also does not provide any information on the dispersity of arms, i.e., the differences in the lengths of arms. It, however, indicates that all initiator arms are esterified such that the majority of the material is comprised of star-shaped PLGA based on the added initiator.

3.3. Confirmation of the presence of the glucose core in Glu-PLGA

The initial ^{13}C NMR spectra of Glu-PLGA in Fig. 3 did not show any peaks related to glucose, and thus, it was necessary to confirm the presence (or the absence) of glucose. The synthesis of Glu-PLGA by ring-opening polymerization was investigated stepwise. DMSO-d6 was used as a solvent for collection of ^{13}C-NMR spectra, as it possessed a good solubility for both glucose and PLGA and the use of a single solvent enables easier comparisons between spectra. The PLGA and glucose spectra are shown in Fig. 4A and B. The naturally occurring peaks in ^{13}C-NMR for PLGA in DMSO-*d*6 are observed at 16–17 ppm, 60–61 ppm, 68–69 ppm, 166–167 ppm, and 169–170 ppm. The glucose ^{13}C NMR has some peaks overlapping with these regions except for peaks notably located at 92–93 ppm and 96–97 ppm. These two peaks, which are prominent in ^{13}C-labeled glucose, were used as the primary means for tracking the glucose presence or its absence for the rest of the assays. Ring-opening polymerization is a high-temperature process which typically involves a hydroxyl-activating catalyst. Morphologically, glucose readily transitions to a brownish-black color under these conditions by a series of oxidation-type reactions. These reactions have been heavily investigated largely in the presence of amino-acids as they relate to food science and the varying mechanisms have been reported previously [45–47]. Similarly, Glu-PLGA adopts this color only reverting to white upon de-colorization using activated charcoal.

Table 2
PLGA standards and samples used for this study.

#	Source, Catalog#	Lot#	L:G*	M_n **	M_w **
Linear PLGA					
1	Akina, AP063, E (= Ester end-cap)	180510RAI-A	54:46	22,779	32,595
2	Akina, AP076, A (= Acid end-cap)	50630MLS	55:45	36,112	51,921
3	Akina, AP222	170921FAJ	56:44	46,961	81,919
4	Akina, AP121	180521RAI-B	53:47	50,589	75,311
5	Akina, AP071	170706AMS-B	100:0	38,513	57,374
6	Evonik, RG502H, IV 0.16–0.24 dL/g, A	D170300516	50:50	7567	12,237
7	Evonik, RG503H, IV 0.32–0.44 dL/g, A	D160900556	50:50	23,747	33,983
8	Evonik, RG504H, IV 0.45–0.60 dL/g, A	D160400525	50:50	40,763	60,889#
9	Evonik, RG653H, IV 0.16–0.24 dL/g, A	D130600518	65:35	22,400	34,944
10	Evonik, R755S, IV 0.50–0.70 dL/g, E	D151200583	75:25	51,168	72,176
11	Evonik, R756S, IV 0.71–1.0 dL/g, E	D150800568	75:25	97,797	107,234
12	Evonik, RG858S, IV 1.3–1.7 dL/g, E	D16100568	85:15	122,496	179,454
13	Evonik, R205S, IV 0.55–0.75 dL/g, E	D161000564	100:0	53,352	76,949
14	Lactel, B6010-2, IV 0.55–0.75 dL/g, E	A17-065	53:47	48,530	69,629
15	Lactel, B6001-1, IV 0.55–0.75 dL/g, E	A14-0796	65:35	35,505	49,850
16	Lactel, B6007-1, IV 0.55–0.75 dL/g, E	A16-160	76:24	55,977	83,973
17	Lactel, B6006-1, IV 0.55–0.75 dL/g, E	A15-051	86:14	50,412	75,554
Branched (or Star-shaped) PLGA					
18	2-arm U-shaped PLGA (Akina, AP245)	180710-RAI-B	55:45	34,201	48,948
19	2-arm U-shaped PLGA (Akina, AP244)	180710-RAI-A	57:43	41,278	59,381
20	3-arm PLGA (Akina, AP229)	171011JSG-A	56:44	44,029	57,854
21	3-arm PLGA (Akina, AP237)	180717FAJ-A	75:25	47,586	59,930
22	4-arm PLGA (Akina, AP227)	171101SLG-B	57:43	47,129	59,686
23	5-arm PLGA (Akina, AP236)	180514RAI-B	53:47	46,028	57,126
24	5-arm PLGA (Akina, AP238)	180716FAJ-A	77:23	53,800	65,607
25	6-arm PLGA (Akina, AP228)	171103SLG-A	56:44	49,576	59,275
26	Glu-PLGA (Akina, ^{13}C for C1 & C2)	180327RAI-A	50:50	19,380	31,604
27	Glu-PLGA (Akina, ^{13}C for C1∼C6)	180608-RAI-C	49:51	12,878	22,139
28	Glu-PLGA (Corbion, PDLG5505G)	1604000475	55:45	44,834	69,351
29	Glu-PLGA (Evonik, 5545 DLG 5GLU)	LP1623	55:45	40,178	62,762
30	Glu-PLGA (Lactel (B6131-1)	A17-160	54:46	37,423	61,005

*Measured by ^1H-NMR; **Measured by GPC-ES; IV = inherent viscosity.
#The prior batch of RG504H used in an earlier study had M_w of 77,954 Da measured by GPC-ES and its lot# is R140800515 [42]. This difference in lots accounts for the different molecular weights as determined by GPC-ES between the two studies. The molecular weight of these polymers by the manufacturer is determined by measuring inherent viscosity, and not by GPC.

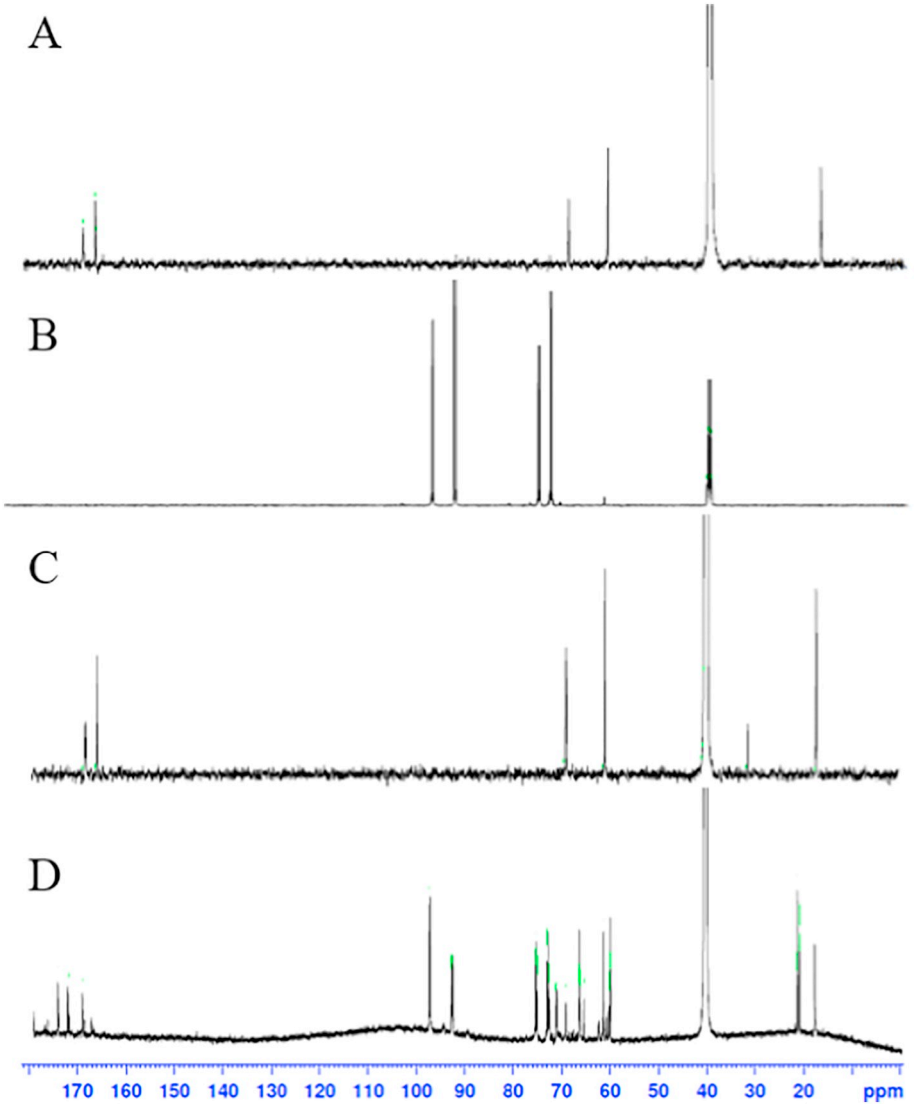

Fig. 4. ^{13}C-NMR Spectra in DMSO-d6 of (A) linear PLGA (Polymer #15), (B) ^{13}C-labeled (C1,2) glucose, (C) ^{13}C-labeled (C1,2) Glu-PLGA (Polymer #26), and (D) Polymer #26 after hydrolysis.

Interestingly, despite the visually obvious color-forming reaction of ^{13}C-labeled glucose, ^{13}C NMR confirmed that the glucose largely survived the polymer synthesis process. The addition of peaks at approximately 32, 30, 25, 23, 14, and 12 ppm are directly attributed to the presence of SnOct, while the formation of a new peak around 177 ppm indicates the formation of a carbonyl group. Despite this, the strong peaks between 70 and 80 and 90–100 ppm indicate that the glucose largely survived this processing. Passively mixing ^{13}C-labeled glucose with loose, linear polymer clearly shows the presence of signature glucose peaks at 90–100 ppm, even when combined at the same weight content as would be theoretically generated in a 50,000 Da PLGA reaction with glucose. This indicates that the presence of PLGA alone does not affect the glucose characteristic peaks. Unlike the physical mixture, however, ^{13}C-labeled Glu-PLGA showed absolutely no glucose peaks (Fig. 4C) even after purification by charcoal to remove the brownish-black color. All peaks were attributable to PLGA. The same results were obtained with the Glu-PLGA synthesized with all 6 ^{13}C-labeled carbons of glucose, as well as the polymer extracted from Sandostatin LAR Depot assayed in $CDCl_3$ (see the Sandostatin LAR NMR characterization section below). In each case, a Glu-PLGA spectrum displays only peaks attributable to PLGA. Additional peaks observed were typically attributable to residual solvents from purification, either hexane (peaks at 14, 23, 32 ppm) or acetone (peaks at 31 ppm, 207 ppm) [44].

Although glucose survives the process of heated stannous-octoate ring-opening polymerization, it is not observed within the Glu-PLGA molecule itself even prior to purification steps which may remove it, or when all 6 carbons are ^{13}C-labeled. There are many potential causes for this including esterification, peak-overlap, or core-shielding [48]. To establish a method for validating the presence of glucose within the molecule, the PLGA chains were hydrolyzed to separate glucose from Glu-PLGA. Accelerated hydrolysis was performed at 50 °C with 100 mg of polymer in 10 mL of 0.1 M NaOH. After 2 months, the aqueous layer was concentrated, re-dissolved in DMSO-d_6 and analyzed by NMR (Fig. 4D). Peaks located at 20, 66, and 176 ppm were attributed to lactic acid, while peaks at 60 and 177 ppm were attributed to glycolic acid [44]. Both of these components would be expected to be observed. For the tested Glu-PLGA with ^{13}C-labeled glucose, the characteristic glucose peaks around 97 and 92 ppm re-appeared indicating that ^{13}C-labeled glucose was released from the Glu-PLGA upon hydrolysis. This further indicates that the glucose is actually present within Glu-PLGA, but in a form or structure which renders it undetectable by ^{13}C-NMR.

3.4. Determination of solvent dn/dc and solvent effect on data quality

Differential refractive index, *dn/dc*, was increased linearly as a function of the PLGA concentration. An important trend noted is that the *dn/dc* value of PLGAs is linearly dependent on the L:G ratio. As previously reported, when the L:G ratio increases, the *dn/dc* value decreases. The linear relationship makes it possible for using accurate *dn/dc* values as long as the L:G ratio is known. This effect occurs in all solvents tested including THF, acetonitrile, and acetone [49]. Due to the low solvent refractive index, acetone also provides nearly a two-fold increase in *dn/dc* relative to THF. Accurate *dn/dc* values are critical for full characterization of PLGA having different L:G ratios. Using accurate *dn/dc* values allows correct interpretation of GPC-4D data regarding the PLGA structures. The *dn/dc* value of the branched standards with the L:G ratio of 55:45 was measured to be around 0.0980 mL/g. It was noted that the branched polymers had a slightly higher *dn/dc* than their linear counterparts (e.g., linear polymer #2 in Table 2 had *dn/dc* of 0.0977 mL/g and 6-arm polymer #25 had *dn/dc* of 0.0980 mL/g). These differences were compensated for within the software.

Initial online analysis with dynamic light scattering (DLS) proved to be implausible using THF as a mobile phase. The decay correlation was nearly flat and the instrumental uncertainty for THF was excessive, ≥80%. Changing to acetone improved the critical parameter of *dn/dc* resulting in a drastic improvement of the decay signal for the Astra QELS experiment. The instrumental uncertainty of the measurement of hydrodynamic radius (R_h) decreased to around 16% when acetone was used at the sample load of 500 µg.

3.5. Determination of sample load on GPC-4D data quality

Various sample loads ranging from 50 µg to 500 µg were tested by altering the sample concentration and injection volume. A 50 µL injection of 2.5 mg/mL (125 µg polymer) solutions proved to be best. The most accurate branch unit per molecule for a 4-arm PLGA (Polymer #22 in Table 2) was obtained with 50 µL injection (the branch unit/molecule of 4.21 ± 0.04). This data was obtained using the viscosity method/star model with a monodisperse slice setting, a drainage factor of 0.75, and with other parameters optimized as detailed in other sections. The sample load also had a direct effect when using the viscosity data for determining the branch units per molecule.

3.6. Osmometer

To ensure that the GPC systems were reporting values in line with an empirical method that is not dependent on standards or models, osmometry was also performed (Table 3). In all cases, the osmometer results either fell within the manufacturer reported accuracy of the osmometer (± 5 kDa) or there was no statistically significant difference between the osmometer results and the M_n indicated by GPC-4D indicating that these results are valid. Since the measurement by osmometer requires a large sample amount, it was used only for two tests on Glu-PLGA extracted from Sandostatin LAR instead of four. The M_n measured by GPC-4D, however, can be used instead of M_n measured by osmometer.

Table 3
Comparison Osmometer data to GPC-4D for indicated polymers.

Polymer	M_w (GPC-4D)	M_n (GPC-4D)	Osmometer M_n (n = 4)
3-Arm PLGA (AP229)	42,010 ± 177	36,714 ± 115	39,464 ± 3129
4-Arm PLGA (AP227)	44,869 ± 395	39,496 ± 438	43,513 ± 1174
6-Arm PLGA (AP228)	49,375 ± 269	46,715 ± 281	51,879 ± 5569
Glu-PLGA (Corbion)	52,148 ± 84	40,985 ± 48	42,440 ± 2093
Glu-PLGA (Evonik)	52,943 ± 306	40,061 ± 466	43,339 ± 2195
Glu-PLGA (Sandostatin LAR)	43,835 ± 1196	37,188 ± 950	39,306 ± 6071

3.7. Intrinsic viscosity for determining the branch units per molecule by GPC-4D

The results of GPC-4D were very sensitive to the system conditions, such as a temperature fluctuation and a mobile phase quality. Thus, experimental conditions were optimized to reduce the variability in system conditions to the minimum. Desiccant packs were added to the mobile phase to help with reduction of water absorbed into the mobile phase from the atmosphere. The MALLS detector was thermally controlled by placing copper-piped heat-exchanger plates above and below it with the detector and exchangers encased in an enclosure comprised of 0.220-in. acrylic sheets. A water recirculator set to 20 °C was attached to the heat exchangers to provide a consistent temperature environment for the MALLS system.

Decreasing the flow rate to 0.3 ml/min provided the ability to obtain R_g, giving an option of determining the branch number by the radius method (Eq. (1) in Table 1). The radii obtained, however, had a much larger variability than the viscosity measurement mainly due to the small size of the polymers examined. Thus, the intrinsic viscosity method was chosen (Eq. (2) in Table 1) for quantifying the branching extent. The viscosity method requires the right drainage factor (Eq. (3) in Table 1) to calculate the right branch units per molecule. The right drainage factor was determined as described below.

3.8. Optimization of parameters for determining the branch units per molecule

Initial work with THF as a mobile phase produced widely different results for the branch unit data which were unreliable due to the poor *dn/dc* and poor ability to dissolve PLGAs with the L:G ratio < 60:40. Although acetone produced improved collection of data from the polymer, the true determination of the branch units requires a relevant linear PLGA of the same molecular weight and the same L:G ratio. Even the PLGA with the L:G ratio of 50:50 (Polymer #8 in Table 2) did not provide accurate measurements of the branch units, despite the same molecular weight range as Glu-PLGA samples. Since the L:G ratio of Glu-PLGA from Sandostatin LAR is 55:45, Polymer #2 in Table 2 was used as a linear standard.

Even the type of the end-cap has an impact on apparent branch units per molecule. When one linear polymer is compared to itself for the branching experiment the result is a flat line with two branch units per molecule across the molar mass distribution. Comparing two different linear PLGAs results in some deviation from two branch units even if there is a slight difference in composition.

Intrinsic viscosity was chosen to quantify the branching extent. To optimize the branching determination, a series of multi-arm PLGAs were synthesized and characterized (Polymers #20, 22, 23, and 25) to confirm full esterification of the initiator as a confirmation of branching. These were used to optimize the parameters used in the calculation of the branch units. Testing the four models of branching (tri-functional, tetra-functional, comb, or star), with a default drainage factor of 1.0, revealed the star model to be the best fit.

After selecting the star model for the method of branching determination, further refinement of the method was performed by examining the drainage factor. The drainage factor is primarily related to how the polymer interacts with the solvent. Specifically, the drainage factor affects the branch units per molecule as described in Eq. (3), $g' = g^e$, in Table 1. There is an inverse relationship between drainage factor and branch units per molecule. As the drainage factor decreases, the branching units per molecule increases. By systematically examining how the drainage factor changes the resultant branch units per molecule relative to nominal, 0.75 was chosen as the best fit across the PLGA branched standards. Fig. 5 shows the calculated branch units for each standard. The upward deviations observed at the higher molecular ends are likely due to the lower concentration of polymers, resulting in inaccurate calculation of the branch units. It is also likely that the

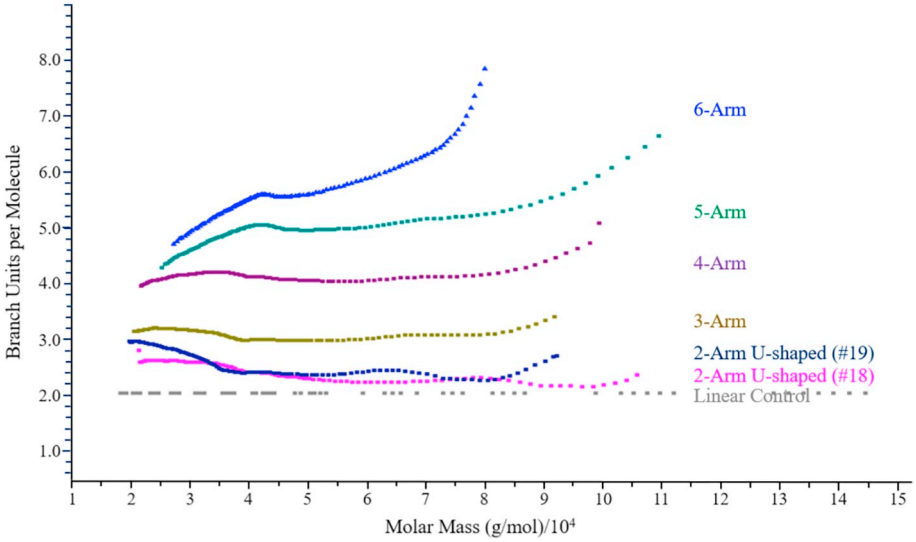

Fig. 5. The branch units per molecule as a function of the molar mass of branched PLGAs with branch units ranging from 2 to 6.

molecules may aggregate to present the branch number higher than individual molecules. The same trend was observed with all samples.

A potential outcome from a partially-esterified glucose molecule (for example at positions 3, 4) would be a 'U-shaped' PLGA in which the chain is largely free, while somewhere within the middle of the polymer there is a constrained location. The ability of the system to detect and analyze such a "U-shape," rather than a true star, polymers on branching units per molecule were also examined. This was done by synthesizing PLGA 55:45 polymers using 1,2,-hexanediol to create a U-shaped polymer chain (Polymers #18 and #19 in Table 2). Fig. 5 shows the results for the U-shaped polymers in comparison with other branched PLGAs (Polymers #20, 22, 23, and 25). The U-shaped PLGA polymers were observed to generate a branching degree intermediate to that of perfectly linear (branch unit of 2.0) and a three-armed star (branch unit of 3.0).

3.9. Determination of the branch units per molecule of Glu-PLGA

The branch units per molecule of Glu-PLGAs that are commercially obtained and extracted from Sandostatin LAR were determined using the method validated above. The calculated branch units of various Glu-PLGAs are shown in Fig. 6, and the summary of the data for branched polymers with optimized chromatographic and software parameters is in Table 4. The branch units of Sandostatin LAR ranges from 2 (i.e., linear) to < 4 as the molecular weight increases from 20,000 Da to 80,000 Da, which constitutes 94% of the total molar mass. Thus, it is safe to conclude that the majority of Sandostatin LAR Glu-PLGA has < 4 branch units. Table 4 shows that the branch unit/Glu-PLGA from Sandostatin LAR is around 3.2.

Another noticeable observation is that the branch units of Glu-PLGAs from Corbion, Evonik, and Lactel are substantially smaller than those of Sandostatin LAR, but the Glu-PLGAs from three commercial sources have substantially higher molecular weights up to 150,000 Da. Sandostatin LAR Glu-PLGAs in Fig. 6 show variations in the branch units, but overall, the branch units per molecule is < 4. The branch unit profiles of Sandostatin LAR Glu-PLGA are very different from those of Corbion, Evonik, and Lactel. It is important to note, however, that the overall Glu-PLGA properties can be changed by various factors during a series of formulation processing steps. This highlights the importance of testing the polymers obtained from the final formulation rather than the raw polymers.

3.10. Mark-Houwink plots of Glu-PLGAs

While the calculation using Eq. (4) of Table 1 provides branch units of Glu-PLGAs as shown in Fig. 6 and Table 4, the values are based on the model, the star model with arms of random length in this case. It also requires identification of accurate drainage factor. The branch units of Glu-PLGAs can be determined without any theoretical model from the Mark-Houwink plots, $[\eta] = KM^{\alpha}$ or $\log[\eta] = \log K + \alpha(\log M)$, where $[\eta]$ and M are intrinsic viscosity and molecular weight, respectively. Fig. 7 shows the Mark-Houwink plots of all branched PLGAs tested. Fig. 7A shows triplicates of each Glu-PLGA, and Fig. 7B shows plots of branch standards including 2-arm U-shape. The intrinsic viscosities of Glu-PLGAs from Sandostatin LAR are compared with those of branch standards of 2–6 arms (Fig. 7C–F). The intrinsic viscosity data clearly indicate that the branch units of Glu-PLGA of the samples tested increase as the molecular weight increases.

Fig. 7C–F presents the plots of Sandostatin LAR samples against the branch standards to make it easier to see the changes in the branch units as the molecular weight increases. The plots of all Sandostatin LAR Glu-PLGAs match with the plot of the branch standard with 2 arms, i.e., linear PLGA, at the lower end of the molecular weight, but they mostly overlap with the 3-arm standard. Only at higher molecular weight end the plot may extend into the 4-arm standard. Most (94%) of the Glu-PLGAs from Sandostatin LAR have the branch units per molecule < 4, and only a small fraction (< 6%) may have the branch unit of 4, although the average branching value ranges from 3.10 to 3.25 for the assayed Sandostatin LAR extracts.

The usefulness of the Mark-Houwink plot is that it can determine the branch units by comparing the intrinsic viscosity of a sample with the branch standards, and the change in branch units is easily seen as the molecular weight increases. The determination of the branch units of samples by the Mark-Houwink plot does not require the drainage factor. Thus, the two methods based on drainage factor and intrinsic viscosity are complementary to each other and provide accurate determination of the branch units of unknown samples. The Glu-PLGAs extracted from Sandostatin LAR have the branch units ranging from 2 to 3, and only a small fraction of high molecular weights may have the branch units of 4. It is safe to conclude that the majority of Glu-PLGAs isolated from Sandostatin LAR have the branch units per molecule < 4.

4. Discussion

4.1. GPC characterization of Glu-PLGA obtained from Novartis

Glu-PLGA from Novartis was analyzed by GPC in a study by Kang

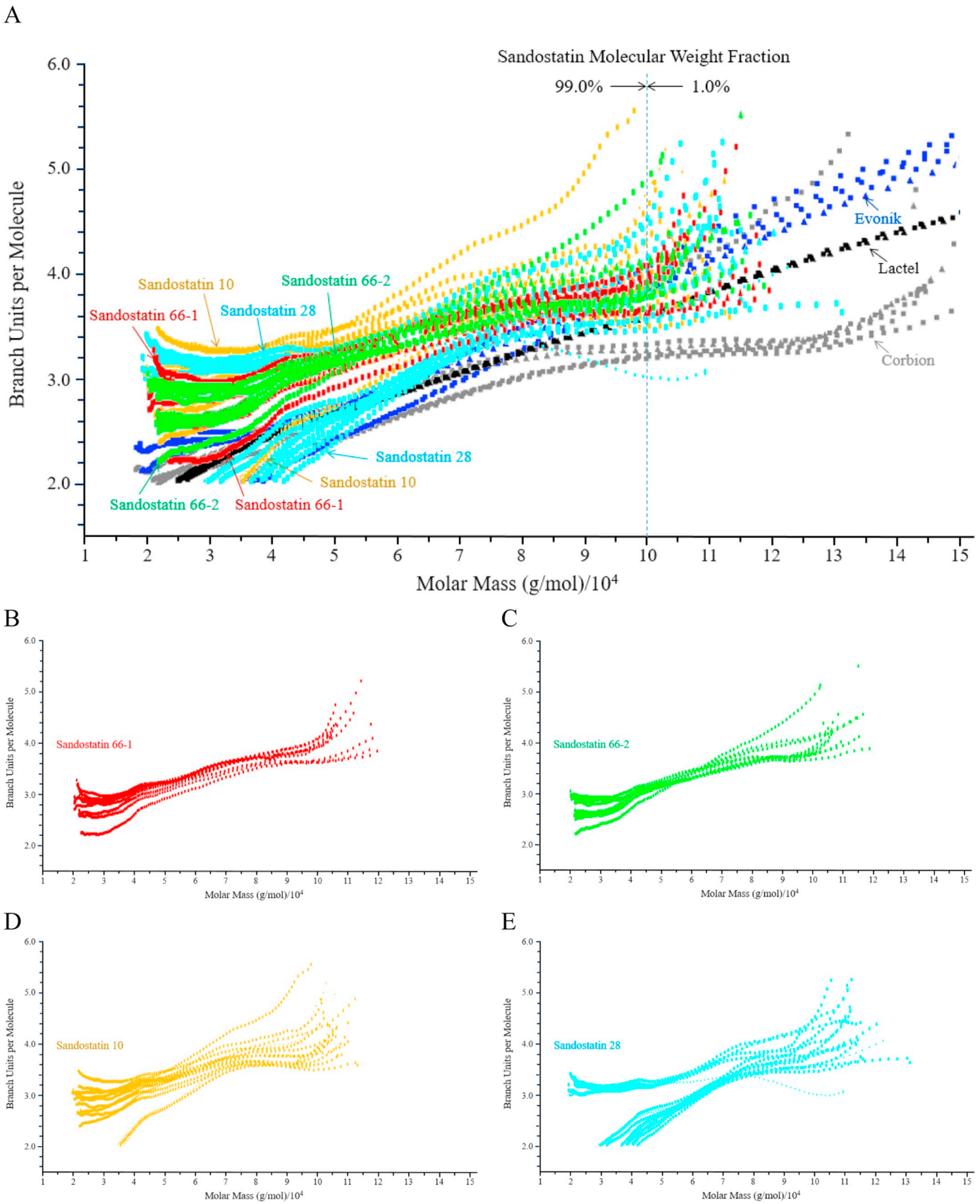

Fig. 6. (A) The branch units per molecule as a function of the molar mass of four Sandostatin LAR extracts from 3 different lots (66: 356166; 10: 356510; and 28: 357028), Corbion, Evonik, and Lactel. (B)~(E) are the individual plots for Sandostatin LAR 356166-1, 356166-2, 356510 and 357028, respectively.

Table 4
GPC-4D data obtained from indicated polymer. (n = 3).

#	Polymer (dn/dc)	Average Branch Units	Branch Units at M_w	Branch Units at M_n	M_n (GPC-4D)	M_w (GPC-4D)	Viscosity at M_n (mL/g)	$R_h(Q)$ at M_n (nm)	$R_h(V)$ at M_n (nm)
18	2-Arm U-shaped PLGA, (AP245) (0.0977 mL/g)	2.56 ± 0.02	2.35 ± 0.02	2.46 ± 0.06	34,230 ± 1126	38,693 ± 788	32.47 ± 0.60	4.20 ± 0.18	5.55 ± 0.10
19	2-Arm U-shaped PLGA, (AP244) (0.0977 mL/g)	2.54 ± 0.23	2.42 ± 0.15	2.51 ± 0.19	40,938 ± 1244	46,301 ± 1063	35.69 ± 0.02	6.96 ± 2.00	6.08 ± 0.07
20	3-Arm PLGA (0.0973 ± 0.0007 mL/g)	3.07 ± 0.06	3.00 ± 0.08	2.97 ± 0.04	36,714 ± 115	42,010 ± 177	32.35 ± 0.11	5.57 ± 1.01	5.66 ± 0.01
22	4-Arm PLGA (0.0980 ± 0.0007 mL/g)	4.31 ± 0.11	4.17 ± 0.03	4.22 ± 0.17	39,496 ± 438	44,869 ± 395	30.80 ± 0.11	4.94 ± 0.22	5.72 ± 0.03
24	5-Arm PLGA (0.0980 mL/g)	5.03 ± 0.02	5.07 ± 0.06	4.98 ± 0.07	44,458 ± 176	48,385 ± 151	30.36 ± 0.07	4.73 ± 0.19	5.94 ± 0.01
25	6-Arm PLGA (0.0980 ± 0.0012 mL/g)	5.65 ± 0.06	5.69 ± 0.05	5.76 ± 0.04	46,715 ± 281	49,375 ± 269	29.37 ± 0.03	5.23 ± 0.19	5.99 ± 0.01
28	Glu-PLGA (Corbion) (0.0996 ± 0.0026 mL/g)	2.85 ± 0.08	2.56 ± 0.16	2.30 ± 0.16	39,525 ± 1608	50,982 ± 1379	36.31 ± 0.13	5.42 ± 0.54	6.06 ± 0.02
29	Glu-PLGA (Evonik) (0.0987 ± 0.0012 mL/g)	3.14 ± 0.19	2.64 ± 0.16	2.32 ± 0.24	39,862 ± 381	52,542 ± 470	35.58 ± 0.35	4.66 ± 0.32	5.97 ± 0.05
30	Glu-PLGA (Lactel) (0.0980 mL/g)	2.99 ± 0.02	2.73 ± 0.01	2.51 ± 0.02	42,469 ± 289	55,049 ± 171	35.93 ± 0.05	5.25 ± 0.58	6.12 ± 0.01
31	Glu-PLGA (Sandostatin 66-1) (0.0980 mL/g)	3.11 ± 0.18	3.07 ± 0.14	2.89 ± 0.18	37,743 ± 510	44,437 ± 816	32.78 ± 0.39	4.80 ± 0.91	5.76 ± 0.05
32	Glu-PLGA (Sandostatin 66-2) (0.0980 mL/g)	3.10 ± 0.09	3.04 ± 0.009	2.83 ± 0.09	37,211 ± 365	43,683 ± 416	32.74 ± 0.43	4.90 ± 0.74	5.72 ± 0.04
33	Glu-PLGA (Sandostatin 10) (0.0980 mL/g)	3.25 ± 0.18	3.07 ± 0.31	2.85 ± 0.41	36,676 ± 1020	43,012 ± 856	32.19 ± 0.75	4.77 ± 0.56	5.67 ± 0.09
34	Glu-PLGA (Sandostatin 28) (0.0980 mL/g)	3.18 ± 0.20	2.75 ± 0.37	2.55 ± 0.49	39,063 ± 1561	46,473 ± 1248	33.97 ± 1.72	5.11 ± 0.82	5.83 ± 0.15

et al. [50]. In the study, the molecular weight of Glu-PLGA was calculated from a relative calibration curve produced with polystyrene standards (Polysciences, Inc., Warrington, PA). Using polystyrene molecules as standards for calculating the molecular weight of Glu-PLGA is bound to be relative at best in providing relative distribution of molecular weights without structural information. The linear PLGA used in the assay by Kang et al. was PLGA with L:G = 50:50 and inherent viscosity of 0.61 dL/g in 1,1,1,3,3-hexafluoro-2-propanol (HFIP) at 30 °C from Birmingham Polymers, Inc. (Birmingham, AL). The PLGA with this inherent viscosity is equivalent to the molecular weight of 40,000 Da [51]. According to the information available at Lactel, the molecular weight was obtained from GPC calibrated with a standard polymer such as polystyrene. Thus, the absolute molecular weight is not known, but it is around 40,000 Da. According to the study, the linear PLGA had a polydispersity of 1.8, while Glu-PLGA from Novartis had a polydispersity of 3.7. However, the study does not provide any information on the branch units per molecule. The most important lesson from the above analysis on Glu-PLGA from Novartis is that the GPC data does not provide any information on the structure of Glu-PLGA. In fact, there is no conclusive evidence demonstrating the presence of Glu-PLGA.

A team of scientists at Novartis compared pharmacokinetic and polymer properties of Sandostatin LAR and other long-acting PLGA formulations delivering octreotide [52]. In their study, the properties of Glu-PLGA was analyzed using GPC with RI detection to determine the molecular weight of Glu-PLGA against polystyrene standards. ^{1}H NMR was used to determine the L:G ratio by dissolving samples in DMSO-d_6. Their results indicate that Glu-PLGA from Novartis has a molecular weight of 52,000 Da and an L:G ratio of 55:45. The calculation of Glu-PLGA by Novartis scientists using GPC calibrated with polystyrene standards provided a molecular weight value, but it is not an absolute value as measured by light scattering. Furthermore, there is no clear evidence distinguishing Glu-PLGA from linear PLGA. This makes it very difficult to characterize the structural properties of Glu-PLGA from Novartis.

4.2. Calculation of the branch units per molecule of Glu-PLGA

4.2.1. Radius of gyration vs intrinsic viscosity

The most important property of Glu-PLGA arises from their molecular architecture having much higher segment densities than their linear homologues of the same molecular weight. Thus, branched polymers exhibit a smaller hydrodynamic volume, which affects their solution properties. The segment density of branched polymers depends on the number of branch units per molecule, B in Eq. (4) in Table 1 [53]. Additionally, branching affects the mean square radius of gyration $< R_b^2 >$ (Eq. (1) in Table 1) [54]. Comparison of $< R_b^2 >$ of Glu-PLGA to that of linear PLGA provides information on the effect of branching on the size of Glu-PLGA. The extent of branching is commonly described by the branching parameter g (also known as contraction factor or shrinking factor) measuring the effect of branching on the size of a molecule, i.e., the mean square radius of gyration $< R_b^2 >$ for a given molecular weight [55–58].

A g value smaller than 1 indicates a decreased radius of gyration due to branching, i.e., increased compactness of the star polymer. The g value is a result of two effects compensating each other, namely, an increasing number of arms (increasing compactness) and an increasing length of arms (decreasing compactness) [59]. For the g index, M_w (from light scattering) can only be compared with R_g when $M_w \approx M_z$. This is the case for a quadruple detection system, because these values are taken from slices of sufficiently narrow distributions as the polymer elutes through the detector [59]. Thus, $< R_g^2 >$ at the same molecular weight for both Glu-PLGA and linear PLGA can be used to obtain detailed structural information of Glu-PLGA. As described above, the molecular weights of Glu-PLGA used in our study, however, was not large enough to accurately measure $< R_g^2 >$ by GPC-4D. The difficulty

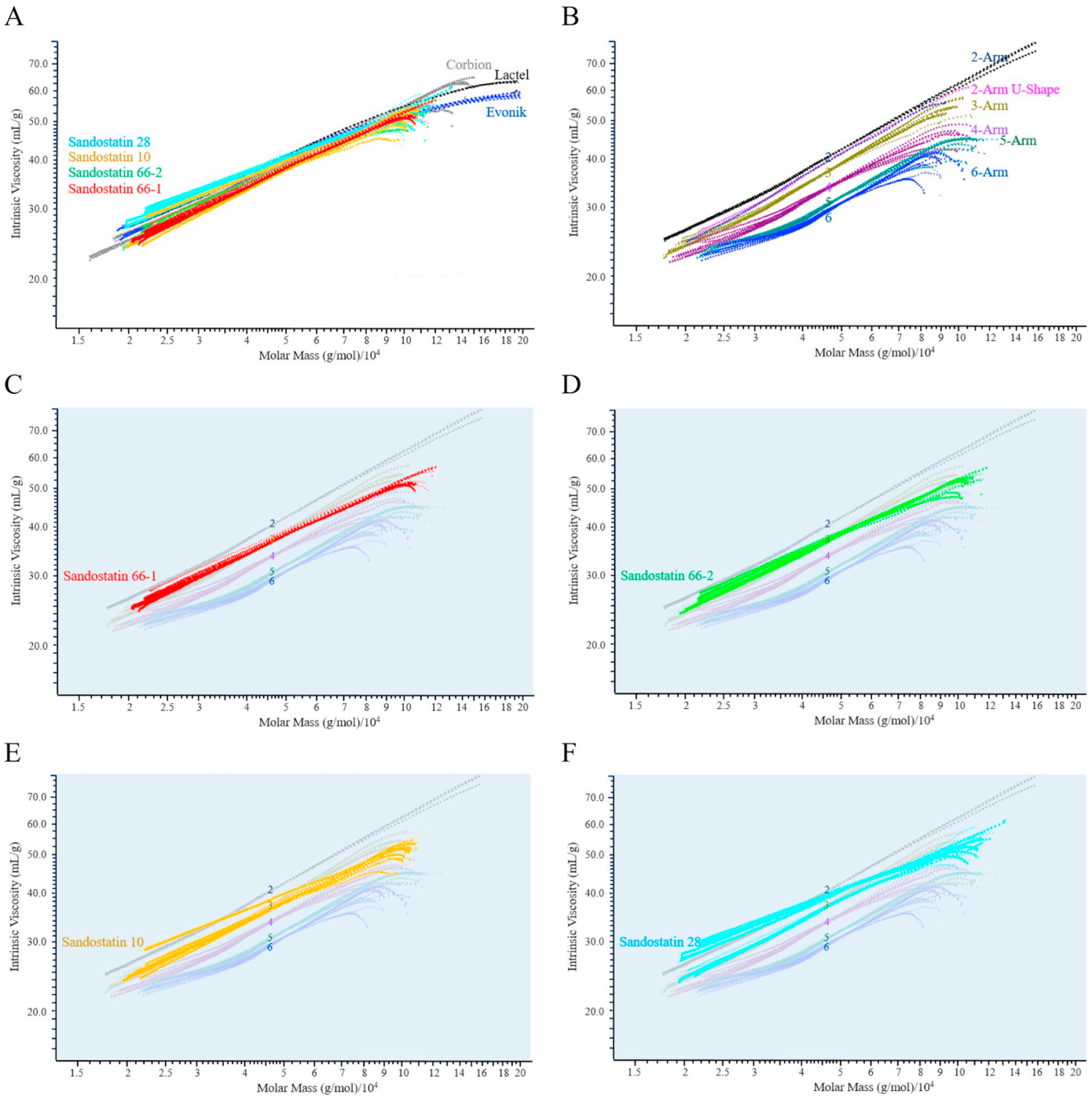

Fig. 7. Mark-Houwink plots of Glu-PLGAs of Sandostatin LAR, Corbion, Evonik, and Lactel (A), branch standards with triplicate measurements of each sample (B), Glu-PLGAs of Sandostatin LAR (lots 356166 (C and D), 356510 (E), and 357028 (F)) in comparison with the branch standards of 2–6 arms.

of determining precise and accurate radius of gyration from GPC-MALLS is not uncommon [54,60].

The intrinsic viscosity [η] has a great advantage for measuring relatively small branched molecules and is an important parameter to be used for characterization of branched polymers in general. The product [η]M is a direct measure of the V_h of a polymer molecule. Even if two different polymers have the same V_h, the molecular weight M and/or [η] of the two can be different. In other words, a linear polymer and a branched polymer may have the same V_h, and cannot be distinguished by GPC, if only V_h is used [61]. Thus, distinguishing Glu-PLGA from linear PLGA, especially when the molecular weights of the two are close, required more extensive characterization. If a Glu-PLGA branched polymer has the same molecular weight as that of a linear polymer, the intrinsic viscosity ratio, $[\eta]_b/[\eta]_l$, is known as the viscometric branching index g' (or branching factor) as shown in Eq. (2) of Table 1. The g' value is obtained from the intrinsic viscosity values, which are experimentally determined without any assumptions [59].

4.2.2. Drainage factor (e)

Drainage factor (e) is a parameter which defines the solvent-polymer interaction including degree of solvation and polymer shape as it relates to the extension of chains. The g' and e are used to calculate the branch units per molecule (Eq. (4) in Table 1). There are different equations available for calculation of the branch units per molecule,

Table 5
Ensemble characterization of Glu-PLGA using 10 parameters.

Parameter	Method	Property
1) L:G ratio	^{1}H-NMR	This affects PLGA properties, in particular, solubility in solvents.
2) Glycolide blockiness (R_c)	$\frac{I_{G-G}}{I_{G-L}}$	This affects solvent solubility.
3) Absolute weight average molecular weight (M_w)	Static light scattering detector with GPC	This is important for the Mark-Houwink plot.
4) Absolute number average molecular weight (M_n)	Osmometer	This value can be replaced with the number average molecular weight (M_n) from GPC.[a]
5) Polydispersity index of Glu-PLGA (PDI_b)	$\frac{M_{w,b}}{M_{n,b}}$	This indicates the broadness of a molecular weight distribution.
6) Molecular weight distribution	GPC with static light scattering detector	This allows calculation of percent fractions of different molecular weights.
7) Intrinsic viscosity ([η])	Online viscometer with GPC	This is essential for the Mark-Houwink plot.
8) Drainage factor (e)	$g' = g^e$	The lower e, the higher branch units.
9) Number of branches (or arms) (B)	$g = \left(\frac{< R_b^2 >}{< R_l^2 >}\right)_M$	This describes the branch units from a glucose core.
10) Polydispersity index of arms ($PDI_{b,arm}$)	$B\left(\frac{M_{w,b}}{M_{n,b}} - 1\right) + 1$	This indicates the heterogeneity of PLGA arms on a glucose core.

[a] Osmometer requires a large amount of a sample which may not be available for clinical formulations.

such as $g = \frac{3B-2}{B^2}$ [62] and $g = \frac{3B}{(B+1)^2}$ [63], depending on the monodisperse or polydisperse branches, but the information on the arm length dispersity of Glu-PLGA is not known, because it is mostly prepared by the core-first method. The lengths of arms are not expected to be identical, but they are not expected to be widely different either. The value of the drainage factor (e) depends on polymer architecture, and thus, could give some additional information on the actual structure of the star-shaped macromolecules. For example, $e = 0.5$ for regular stars and $e = 1.5$ for *comb*-like branched polymers. Stars of intermediate branching have e values between these two [64]. For example, $e = 0.8$ indicates that the structure is closer to the regular star than to highly branched irregular stars with a high distribution of the branch length [59]. The best drainage factor (e) for Glu-PLGA was 0.75, and this indicates that the lengths of PLGA branches in Glu-PLGA are close.

4.2.3. The Polydispersity Index of arms of branched Glu-PLGA ($PDI_{b,arm}$)

Regular star molecules have B linear chains of exactly the same length attached to a B-functional central unit [65]. The branches are expected to be flexible in suitable solvents, and thus, can be described in a first approximation by Gaussian chain statistics [65]. When the branches grow from the core, the polymerization kinetics may follow that of linear chain polymerization, under the spatial confinement exerted by the core. Thus, the length of each arm may be different from each other.

Star-shaped polymers are known to have a lower polydispersity index than the most probable distribution value of 2. The polydispersity index of the star polymers with B branches is related to the polydispersity index of the branches of the star polymer as follows [65–68]:

$$\frac{M_{w,b}}{M_{n,b}} = 1 + \frac{1}{B}\left(\frac{M_{w,arm}}{M_{n,arm}} - 1\right)$$

where $M_{w,arm}$ and $M_{n,arm}$ are weight and number average molecular weights of arms, respectively. For Glu-PLGA synthesized by the core-first method, the values of $M_{w,arm}$ and $M_{n,arm}$ are not known, but the ratio can be calculated by rearranging the above equation to:

$$\frac{M_{w,arm}}{M_{n,arm}} = B\left(\frac{M_{w,b}}{M_{n,b}} - 1\right) + 1$$

here, the ratio $M_{w,arm}/\ M_{n,arm}$ is defined as the polydispersity index of arms ($PDI_{b,arm}$) in Glu-PLGA. The above equation allows estimation of the $PDI_{b,arm}$, as the absolute values of $M_{w,b}$ and $M_{n,b}$ are obtained from light scattering and osmometry. The value can be compared with the polydispersity index of linear PLGA chains to examine whether the chain growth from the glucose core has any impact on the arm length due to the confined structure around the glucose core.

Glu-PLGA of Sandostatin LAR 66-1 (Polymer #31 in Table 4) has the $M_{n,b}$ and $M_{w,b}$ of 37,743 and 44,437, respectively. Thus, the polydispersity index of arms of Glu-PLGA is calculated to be 1.58. This polydispersity index of arms matches with the drainage factor of 0.75, indicating a star shape structure. The polydispersity index of arms, however, is larger than the polydispersity index of the Glu-PLGA itself.

$$\frac{M_{w,arm}}{M_{n,arm}} = 3.11\left(\frac{44{,}437}{37{,}743} - 1\right) + 1 = 1.55$$

The polydispersity indexes of other three Sandostatin LAR Glu-PLGAs are 1.54, 1.56, and 1.60 for Polymer #32, 33, and 34, respectively. All branched polymers listed in Table 4 have the polydispersity index between 1.33 and 1.76. The PLGAs with 2–6 arms (Polymers #18–25 in Table 8) have the polydispersity index in the range of 1.33–1.56, while Glu-PLGAs from Corbion, Evonik, and Lactel have 1.82, 2.00, and 1.89, respectively. It appears that Sandostatin LAR Glu-PLGAs have much lower polydispersity index of arms than other commercial Glu-PLGAs. This sensitive assay enables determination of minute differences among different Glu-PLGAs. However, it does not designate the source of Glu-PLGA used in the Sandostatin LAR formulation. Regardless, this points to the importance of assaying PLGAs from the final formulations.

4.3. Ensemble characterization of Glu-PLGAs

This study has developed an assay method that can recognize unique properties through ensemble characterization of each PLGA, including Glu-PLGA that is used in Sandostatin LAR delivering octreotide acetate. Our study identified 10 parameters that can identify the uniqueness of each PLGA and distinguish different PLGAs. One of the most important parameters is the L:G ratio. It determines the solvent solubility of PLGAs, and thus, other properties. The parameters relevant to Glu-PLGA are listed in Table 5. It is important to measure the absolute molecular weight of Glu-PLGA using static light scattering, and it can be used to obtain a Mark-Houwink plot which is unique, like a fingerprint, for each polymer. The absolute molecular weight is also critical in calculating the number of branches (or arms) per molecule using a drainage factor. All parameters in Table 5 are useful in comparing different Glu-PLGAs, but the three most important parameters are L:G ratio, absolute weight average molecular weight (M_w), and intrinsic viscosity ([η]), which provide the minimum fingerprint characterization of each Glu-PLGA.

5. Conclusion

The goal of this study was to develop analytical techniques to

determine the branch units of Glu-PLGA. Glu-PLGA has been used in Sandostatin LAR, but it has not been thoroughly characterized. The feasibility of glucose-initiated PLGA synthesis has been established and confirmed using ^{13}C-labeled glucose to track its fate through synthesis, purification, and subsequent hydrolysis. A series of branched PLGAs with known branch units per molecule were synthesized and confirmed the branch units using GPC-4D. This method was used to characterize, in particular, to determine the branch units per glucose molecule of Glu-PLGA extracted from Sandostatin LAR, as well as those obtained from commercial sources. The methods in this study can be used to characterize Glu-PLGA for the quality control and Q1/Q2 assessment of the same polymer.

Acknowledgements

This work was supported by Broad Agency Announcement (BAA) Contract # HHSF223201710123C from the Office of Research and Standards/Office of Generic Drugs (OGD) in the FDA. The content is solely the responsibility of the authors and does not necessarily represent the official views of the FDA. The authors would like to acknowledge Dr. John Harwood, Director of the Purdue Interdepartmental NMR Facility, for his support to this work. The support by the Showalter Research Trust Fund is also acknowledged.

References

[1] CDER/Lupron, Approval Package for Lupron Depot, 4 months, 30 mg, Leuprolide Acetate, Application Number: 020517/S002, 1997. http://www.accessdata.fda.gov/drugsatfda_docs/nda/97/020517_s002ap.pdf.
[2] AstraZeneca, NDA 020578/S-032. Zoladex (Goserelin Acetate Implant) 10.8 mg. Highlights of Prescribing Information, https://www.accessdata.fda.gov/drugsatfda_docs/label/2011/020578s032lbl.pdf, (2010).
[3] Novartis, Sandostatin® LAR Depot (Octreotide Acetate for Injectable Suspension), https://www.pharma.us.novartis.com/sites/www.pharma.us.novartis.com/files/sandostatin_lar.pdf, (1998).
[4] Genentech, Nutropin Depot™ [Somatropin (rDNA Origin) for Injectable Suspension], http://www.accessdata.fda.gov/drugsatfda_docs/label/2004/21075s008lbl.pdf, (2004).
[5] CDER/Trelstar, Trelstar LA (Triptorelin Pamoate Lyophilized, 22.5 mg). Approval Package for NDA 22-437, https://www.accessdata.fda.gov/drugsatfda_docs/nda/2010/022437Orig1s000chemr.pdf, (2009) https://www.accessdata.fda.gov/drugsatfda_docs/nda/2010/022437Orig1s000clinpharmr.pdf.
[6] QLT-USA. Eligard® 7.5 mg, 22.5 mg, 30 mg, 45 mg. Leuprolide Acetate for Injectable Suspension. (2007) https://www.accessdata.fda.gov/drugsatfda_docs/label/2007/021731s005,021488s010,021379s010,021343s015lbl.pdf.
[7] Alkermes, RISPERDAL CONSTA® (Risperidone Long Acting Injection) 12.5, 25, 37.5, and 50 mg/vial, https://pdf.hres.ca/dpd_pm/00040784.PDF, (2017).
[8] Alkermes, Vivitrol® (Naltrexone for Extended-Release Injectable Suspension) 380 mg/vial. Package Insert, (2015).
[9] Flexion, ZILRETTA® (Triamcinolone Acetonide Extended-Release Injectable Suspension) for Intra-Articular Use; 32 mg/vial, https://www.accessdata.fda.gov/drugsatfda_docs/label/2017/208845s000lbl.pdf, (2017).
[10] N. Faisant, J. Siepmann, J.P. Benoit, PLGA-based microparticles: elucidation of mechanisms and a new, simple mathematical model quantifying drug release, Eur. J. Pharm. Sci. 15 (2002) 355–366.
[11] C. He, S.W. Kim, D.S. Lee, In situ gelling stimuli-sensitive block copolymer hydrogels for drug delivery, J. Control. Release 127 (2008) 189–207.
[12] H. Seyednejad, A.H. Ghassemi, C.F. van Nostrum, T. Vermonden, W.E. Hennink, Functional aliphatic polyesters for biomedical and pharmaceutical applications, J. Control. Release 152 (2011) 168–176.
[13] K.N. Kang, D.Y. Kim, S.M. Yoon, J.S. Kwon, H.W. Seo, E.S. Kim, B. Lee, J.H. Kim, B.H. Min, H.B. Lee, M.S. Kim, In vivo release of bovine serum albumin from an injectable small intestinal submucosa gel, Int. J. Pharm. 420 (2011) 266–273.
[14] A. Rawat, U. Bhardwaj, D.J. Burgess, Comparison of in vitro–in vivo release of Risperdal® Consta® microspheres, Int. J. Pharm. 434 (2012) 115–121.
[15] C. Regnier-Delplace, O. Thillaye du Boullay, F. Siepmann, B. Martin-Vaca, N. Degrave, P. Demonchaux, O. Jentzer, D. Bourissou, J. Siepmann, PLGA microparticles with zero-order release of the labile anti-Parkinson drug apomorphine, Int. J. Pharm. 443 (2013) 68–79.
[16] S.P. Schwendeman, R.B. Shah, B.A. Bailey, A.S. Schwendeman, Injectable controlled release depots for large molecules, J. Control. Release 190 (2014) 240–253.
[17] H. Gasmi, F. Danede, J. Siepmann, F. Siepmann, Does PLGA microparticle swelling control drug release? New insight based on single particle swelling studies, J. Control. Release 213 (2015) 120–127.
[18] A. Jain, K.R. Kunduru, A. Basu, B. Mizrahi, A.J. Domb, W. Khan, Injectable formulations of poly(lactic acid) and its copolymers in clinical use, Adv. Drug Del. Rev. 107 (2016) 213–227.
[19] H. Gasmi, F. Siepmann, M.C. Hamoudi, F. Danede, J. Verin, J.F. Willart, J. Siepmann, Towards a better understanding of the different release phases from PLGA microparticles: dexamethasone-loaded systems, Int. J. Pharm. 514 (2016) 189–199.
[20] A. Jahandideh, K. Muthukumarappan, Star-shaped lactic acid based systems and their thermosetting resins; synthesis, characterization, potential opportunities and drawbacks, Eur. Polym. J. 87 (2017) 360–379.
[21] H. Wang, G. Zhang, X. Ma, Y. Liu, J. Feng, K. Park, W. Wang, Enhanced encapsulation and bioavailability of breviscapine in PLGA microparticles by nanocrystal and water-soluble polymer template techniques, Eur. J. Pharm. Biopharm. 115 (2017) 177–185.
[22] A. Michalski, M. Brzezinski, G. Lapienis, T. Biela, Star-shaped and branched polylactides: synthesis, characterization, and properties, Prog. Polymer Sci. 89 (2019) 159–212.
[23] C. Bode, H. Kranz, F. Siepmann, J. Siepmann, In-situ forming PLGA implants for intraocular dexamethasone delivery, Int. J. Pharm. 548 (2018) 337–348.
[24] H. Kamali, E. Khodaverdi, F. Hadizadeh, S.A. Mohajeri, In-vitro, ex-vivo, and in-vivo evaluation of buprenorphine HCl release from an in situ forming gel of PLGA-PEG-PLGA using N-methyl-2-pyrrolidone as solvent, Mater. Sci. Eng. C 96 (2019) 561–575.
[25] C. Regnier-Delplace, O. Thillaye du Boullay, F. Siepmann, B. Martin-Vaca, P. Demonchaux, O. Jentzer, F. Danède, M. Descamps, J. Siepmann, D. Bourissou, PLGAs bearing carboxylated side chains: novel matrix formers with improved properties for controlled drug delivery, J. Control. Release 166 (2013) 256–267.
[26] R. Mazarro, L.I. Cabezas, A. De Lucas, I. Gracia, J.F. Rodriguez, Study of different catalysts and initiators in bulk copolymerization of d, l-lactide and glycolide, J. Macromol. Sci. Part A: Pure Appl. Chemistry 46 (2009) 1049–1059.
[27] S.J. Lee, B.R. Han, S.Y. Park, D.K. Han, S.C. Kim, Sol-gel transition behavior of biodegradable three-arm and four-arm star-shaped PLGA-PEG block copolymer aqueous solution, J. Polym. Sci. Part A: Polym. Chem. 44 (2006) 888–899.
[28] S. Davaran, Y. Omidi, M.R. Rashidi, M. Anzabi, A. Shayanfar, S. Ghyasvand, N. Vesal, F. Davaran, Preparation and in vitro evaluation of linear and star-branched PLGA nanoparticles for insulin delivery, J. Bioact. Compat. Polym. 23 (2008) 115–131.
[29] J. Garner, S. Skidmore, H. Park, K. Park, S. Choi, Y. Wang, A protocol for assay of poly (lactide-co-glycolide) in clinical products, Int. J. Pharm. 495 (2015) 87–92.
[30] A.G. Hausberger, P.P. DeLuca, Characterization of biodegradable poly (D,L-lactide-co-glycolide) polymers and microspheres, J. Pharm. Biomed. Anal. 13 (1995) 747–760.
[31] R. d'Arcy, J. Burke, N. Tirelli, Branched polyesters: preparative strategies and applications, Adv. Drug Del. Rev. 107 (2016) 60–81.
[32] M.I. Malik, H. Pasch, Field-flow fractionation: new and exciting perspectives in polymer analysis, Prog. Polym. Sci. 63 (2016) 42–85.
[33] M.D.P. Buera, J. Chirife, S.L. Resnik, R.D. Lozano, Nonenzymatic browning in liquid model systems of high water activity: kinetics of color changes due to caramelization of various single sugars, J. Food Sci. 52 (1987) 1059–1062.
[34] D.D. Bly, Resolution and fractionation in gel permeation chromatography, J. Polymer Sci. Part C (1968) 13–21.
[35] M. Potschka, Universal calibration of gel permeation chromatography and determination of molecular shape in solution, Anal. Biochem. 162 (1987) 47–64.
[36] N. O'brien, A. McKee, D.C. Sherrington, A.T. Slark, A. Titterton, Facile, versatile and cost effective route to branched vinyl polymers, Polymer 41 (2000) 6027–6031.
[37] W.-J. Wang, S. Kharchenko, K. Migler, S. Zhu, Triple-detector GPC characterization and processing behavior of long-chain-branched polyethylene prepared by solution polymerization with constrained geometry catalyst, Polymer 45 (2004) 6495–6505.
[38] W. Prikoszovich, Purified Polylactide and Pharmaceutical Composition Thereof, (1990).
[39] J. Garner, D. Davidson, G.J. Eckert, C.T. Barco, H. Park, K. Park, Reshapable polymeric hydrogel for controlled soft-tissue expansion: in vitro and in vivo evaluation, J. Control. Release 262 (2017) 201–211.
[40] J. Garner, S. Skidmore, H. Park, K. Park, S. Choi, Y. Wang, Beyond Q1/Q2: the impact of manufacturing conditions and test methods on drug release from PLGA-based microparticle depot formulations, J. Pharm. Sci. 107 (2018) 353–361.
[41] J. Burke, R. Donno, R. d'Arcy, S. Cartmell, N. Tirelli, The effect of branching (star architecture) on poly(D,L-lactide)(PDLLA) degradation and drug delivery, Biomacromolecules 18 (2017) 728–739.
[42] S. Skidmore, J. Hadar, J. Garner, H. Park, K. Park, Y. Wang, X.J. Jiang, Complex sameness: separation of mixed poly(lactide-co-glycolide)s based on the lactide:glycolide ratio, J. Control. Release 300 (2019) 174–184.
[43] R.J. Abraham, M. Mobli, Modelling 1H NMR Spectra of Organic Compounds: Theory, Applications and NMR Prediction Software, John Wiley & Sons, Chichester, UK, 2008 (380 pages).
[44] AIST, Welcome to Spectral Database for Organic Compounds, SDBS, https://sdbs.db.aist.go.jp, (2018).
[45] E.L. Richards, Non-enzymic browning: the reaction between d-glucose and glycine in the `dry' state, Biochem. J. 64 (1956) 639–644.
[46] M. Namiki, Chemistry of Maillard reactions: recent studies on the browning reaction mechanism and the development of antioxidants and mutagens, Adv. Food Res. 32 (1988) 115–184.
[47] D.G. Dyer, J.A. Blackledge, S.R. Thorpe, J.W. Baynes, Formation of pentosidine during nonenzymatic browning of proteins by glucose. Identification of glucose and other carbohydrates as possible precursors of pentosidine in vivo, J. Biol. Chem. 266 (1991) 11654–11660.
[48] Q. Zhang, A. Wang, Y. Meng, T. Ning, H. Yang, L. Ding, X. Xiao, X. Li, NMR method for accurate quantification of polysorbate 80 copolymer composition, Anal. Chem. 87 (2015) 9810–9816.
[49] J. Hadar, J. Garner, S. Skidmore, H. Park, K. Park, Y.K. Jhon, Y. Wang, Correlation

analysis of refractive index (dn/dc) for PLGAs with different ratios of lactide to glycolide, 2018 Controlled Release Society (CRS) Annual Meeting New York, NY, 2018 Abstract 95 https://akinainc.com/pdf/2018CRS-1.pdf.
[50] J. Kang, O. Lambert, M. Ausborn, S.P. Schwendeman, Stability of proteins encapsulated in injectable and biodegradable poly(lactide-co-glycolide)-glucose millicylinders, Int. J. Pharm. 357 (2008) 235–243.
[51] Lactel, Inherent Viscosity Vs. Molecular Weight, http://www.absorbables.com/technical/inherent_viscosity.html, (2019) http://www.absorbables.com/products/standard.html.
[52] H. Petersen, J.-C. Bizec, H. Schuetz, M.-L. Delportr, Pharmacokinetic and technical comparison of Sandostatin® LAR and other formulations of long-acting octreotide, BMC Res. Notes 4 (344) (2011) 1–8.
[53] C. Tsitsilianis, A. Ktoridis, Determination of branching of star-shaped macromolecules by gel-permeation chromatography, Macromol. Rapid Comm. 15 (1994) 845–850.
[54] S. Podzimek, Characterization of branched polymers, Light Scattering, Size Exclusion Chromatography and Asymmetric Flow Field Flow Fractionation, John Wiley & Sons, 2011, pp. 307–345.
[55] A. Lederer, W. Burchard, Hyperbranched Polymers. Macromolecules in between Deterministic Linear Chains and Dendrimer Structures, Royal Society of Chemistry, Cambridge, UK, 2015 (285 pages).
[56] T. Jocks, D. Roessner, Absolute molar mass characterisation, G.I.T. Lab. J. 7–8 (2008) 40–42.
[57] P.J. Wyatt, Light scattering and the absolute characterization of macromolecules, Anal. Chim. Acta 272 (1993) 1–40.
[58] Wyatt-Technology-Corp, Star-branched polymers, The Applications Book, 2002 (42 pages).
[59] G. Lapienis, S. Penczek, Reaction of oligoalcohols with diepoxides: an easy, one-pot way to star-shaped, multibranched polymers. II. Poly(ethylene oxide) stars—-synthesis and analysis by size exclusion chromatography triple-detection method, J. Polym. Sci. Part A 42 (2004) 1576–1598.
[60] T. Pathaweeisariyakul, K. Narkchamnan, B. Thitisak, W. Rungswang, W.W. Yau, An alternative method for long chain branching determination by triple-detector gel permeation chromatography, Polymer 107 (2016) 122–129.
[61] Z. Grubisic, P. Rempp, H. Benoit, A universal calibration for gel permeation chromatography, Polymer Lett. 5 (1967) 735–759.
[62] B.H. Zimm, W.H. Stockmayer, The dimensions of chain molecules containing branches and rings, J. Chem. Phys. 17 (1949) 1301–1314.
[63] W. Burchard, Static and dynamic light scattering from branched polymers and biopolymers, Adv. Polym. Sci. 48 (1983) 1–124.
[64] J. Lesec, M. Millequant, Analysis of star-branched polymers with triple detection (refractive index, viscometry, light scattering) gel permeation chromatography, Int. J. Polymer Anal. Character. 2 (1996) 305–321.
[65] W. Burchard, Solution properties of branched macromolecules, Adv. Polym. Sci. 143 (1999) 113–194.
[66] J.R. Schaefgen, P.J. Flory, Synthesis of multichain polymers and investigation of their viscosities, J. Am. Chem. Soc. 70 (1948) 2709–2718.
[67] H. Gao, Development of star polymers as unimolecular containers for nanomaterials, Macromol. Rapid Commun. 33 (2012) 722–734.
[68] T.G. Wright, W. Weber, H. Pfukwa, H. Pasch, Synthesis and characterization of four-arm star polystyrene based on a novel tetrafunctional RAFT agent, Macromol. Chem. Phys. 216 (2015) 1562–1572.